Langmuir

Article

pubs.acs.org/Langmuir

Probing the Dynamic Nature of DNA Multilayer Films Using Förster Resonance Energy Transfer

Lillian Lee, Angus P. R. Johnston, and Frank Caruso*

Department of Chemical and Biomolecular Engineering, The University of Melbourne, Victoria 3010, Australia

Supporting Information

ABSTRACT: DNA films are of interest for use in a number of areas, including sensing, diagnostics, and as drug/gene delivery carriers. The specific base pairing of DNA materials can be used to manipulate their architecture and degradability. The programmable nature of these materials leads to complex and unexpected structures that can be formed from solution assembly. Herein, we investigate the structure of DNA multilayer films using Förster resonance energy transfer (FRET). The DNA films are assembled on silica particles by depositing alternating layers of homopolymeric diblocks (poly$A_{15}G_{15}$ and poly$T_{15}C_{15}$) with fluorophore (poly$A_{15}G_{15}$-TAMRA) and quencher (poly$T_{15}C_{15}$-BHQ2) layers incorporated at predesigned locations throughout the films. Our results show that DNA films are dynamic structures that undergo rearrangement. This occurs when the multilayer films are perturbed during new layer formation through hybridization but can also take place spontaneously when left over time. These films are anticipated to be useful in drug delivery applications and sensing applications.

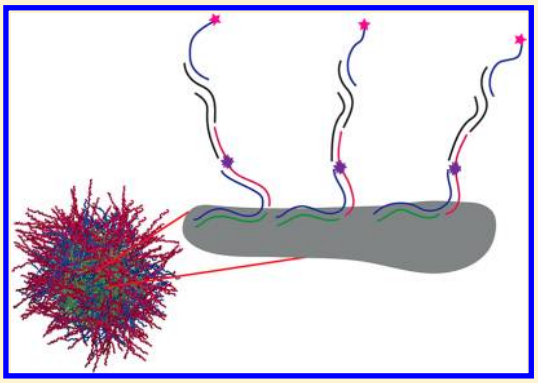

INTRODUCTION

Deoxyribonucleic acid (DNA) is a unique building block, as it exhibits highly precise and specific base pairing interactions between its complementary base pairs. Thus, it can be used to engineer thin films with tunable architectures for potential application in areas such as diagnostics, sensing, and therapeutic delivery. As the architecture of the films plays an important role in the function and response of the material, it is important to understand the structure of the assembled films. DNA films with varying properties can be prepared using the layer-by-layer (LbL) approach,[1] which is widely known as a versatile method for assembling thin films of diverse composition on various supports of different shapes and sizes.[2−7] Through careful selection of the appropriate interactions (e.g., electrostatics,[1] hydrogen bonding,[8,9] and covalent linkages[10,11]), a plethora of building blocks such as polymers,[3] particles,[12] liposomes,[13] micelles,[14] and/or quantum dots[15] can be used to assemble LbL films. In the case of DNA, multilayer films are assembled by depositing alternating layers of diblock DNA held together through the hybridization forces between the complementary blocks in each layer.[16,17] In earlier studies, we demonstrated that DNA film properties are highly dependent on the sequences used for assembly as well as the assembly conditions. For example, through a combination of molecular modeling and experimental measurements, we found that DNA building blocks that are too short (less than 10 bases) or too long (more than 60 bases) do not promote efficient film growth. For short sequences (10 bases long) this is due to the formation of hairpins and for long sequences (60 bases long) it is due to interstrand bridges with adjacent DNA strands, thus preventing efficient hybridization and film growth.[18,19] The presence of salt is also important in forming and stabilizing DNA multilayer films, and at high salt concentrations (2 M NaCl) the formation of T·A*T triplexes results in a denser film structure.[20] DNA multilayer films can also be stabilized by cross-linking the film by hybridization with a specific cross-linking oligonucleotide, thus ensuring the film is still solely composed of DNA.[21] DNA films, including those that are stabilized, can be enzymatically degraded using restriction enzymes by engineering restriction cut sites within the DNA sequences used to assemble the film.[22]

In our previous studies, we reported that slippage plays an important role in the assembly of DNA diblock multilayer films, suggesting a dynamic film structure.[16,17] Rearrangement within LbL films has been extensively studied, and it is well established that polyelectrolyte multilayers consist of interpenetrated rather than stratified layers due to rearrangement within the films.[3,23−26] The chain segments from a polymer have been reported to cross all layers within superlinearly growing films[25] and ∼12 Å between neighboring polymer layers in polystyrensulfonate (PSS)/poly(allylamine hydrochloride) (PAH) multilayer films.[26] The interdiffusion and exchange of the polyelectrolytes within the multilayer films have been attributed to various factors such as the permeability of the film,[27] the presence of salt within the film,[28,29] and the molecular weight of the polyelectrolytes.[30] While rearrangement can lead to nonstratified layers, this can result in useful structures. For

Received: June 26, 2012
Revised: July 25, 2012
Published: August 13, 2012

Scheme 1. (a) Assembly of DNA Multilayer Films on Amine-Functionalized Silica Particles with DNA Diblocks and (b) an Illustration of the Buildup of Layers[a]

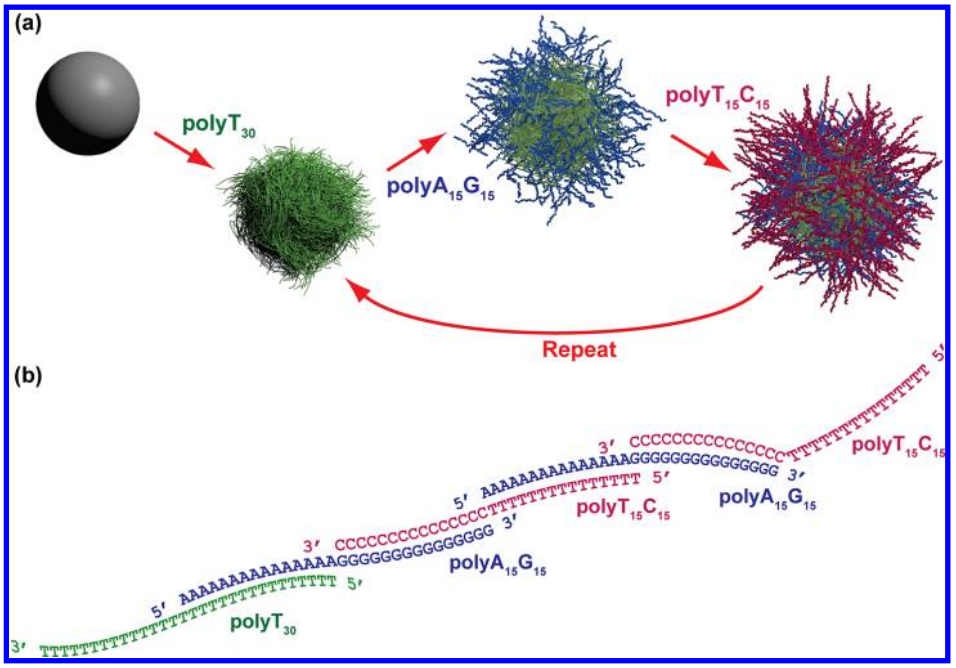

[a]A layer of $polyT_{30}$ is first deposited as a priming layer followed by alternating layers of $polyA_{15}G_{15}$ and $polyT_{15}C_{15}$.

Scheme 2. DNA Multilayer Films with (a) a Terminating AG-F Layer after the Deposition of *a* Layers, Where *a* = 0, 2, 4, 6, or 8; (b) Varying Number of Spacer Layers between the TC-Q and AG-F Layer, Where *a* = 0, 2, 4, 6, or 8; (c) *b* Number of Layers above the Quenched AG-F Layer, Where *b* = 0, 1, 2, 3, 4, 5, 6, or 7; and (d) *a* Number of Spacer Layers between the TC-Q and AG-F Layers, Where *a* = 0, 2, 4, 6, 8 with *b* Number of Layers above the TC-Q and AG-F Layers, Where *b* = 0, 2, 4, 6, or 8[a]

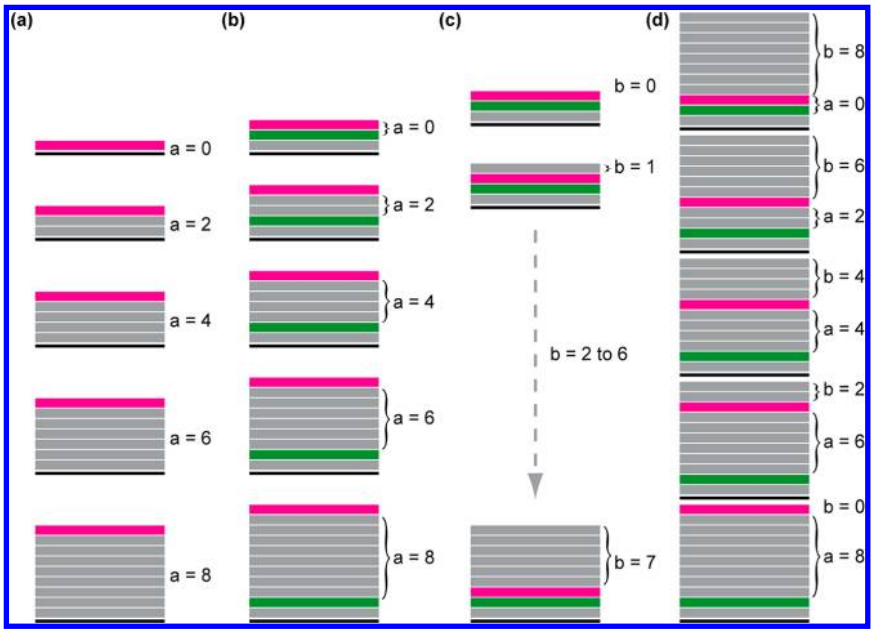

[a]The $polyT_{30}$, TC-Q, and AG-F layers are represented by black, green, and pink lines, respectively. Nonfluorescent layers are represented by gray lines. The number of nonfluorescent spacer layers below the AG-F layer and above the AG-F layer is defined as *a* and *b*, respectively. The TC-Q layer is deposited on a $polyT_{30}/polyA_{15}G_{15}$ bilayer in (b), (c), and (d).

example, competitive diffusion during the assembly of electrostatically assembled multilayer films was used to spontaneously order virus particles.[31] Hence, by understanding the factors that influence the rearrangement and movement of DNA strands within the film, we expect to be able to engineer DNA films with adaptable properties. This will be useful for applications such as in sensing or drug delivery. For example, a dynamic sensing film would not only facilitate the entry and exit of probes without causing damage to the film, it would also enable easy separation of the probes so the film can be reused multiple times. In drug delivery, rearrangement within the film could be useful in triggering therapeutic delivery. Thus, in this article, we

dx.doi.org/10.1021/la302587t | *Langmuir* 2012, 28, 12527−12535

examine the rearrangement of DNA films using Förster resonance energy transfer (FRET).

FRET is defined as the nonradiative transfer of energy from an excited molecular fluorophore (donor) to another molecular fluorophore (acceptor) with fluorescence emission of the acceptor fluorophore.[32] One primary condition for successful FRET is overlap between the donor emission and acceptor excitation spectrum, which generally occurs when the donor and acceptor are physically less than 10 nm apart.[32,33] The efficiency of the process is distance-dependent and generally decreases at increased distances. The sensitivity of FRET over this range makes it useful as a spectroscopic ruler for the measurement of intramolecular and intermolecular distances.[34]

FRET has been used to study the properties of LbL assemblies.[35−39] Using rhodamine B-labeled melamine formaldehyde particles (acceptor) coated with a PSS and PAH multilayer film, FRET between 6-carboxyfluorescein (donor) in aqueous solution and the LbL film-coated particles was demonstrated. It was shown that FRET could be used to study the properties of the film through the site accessibility of 6-carboxyfluorescein on the surface or within the film and to gain an understanding on the permeability properties of the film.[36] In another study by Richter and Kirstein using alternating layers of PSS and PAH assembled between a single donor layer of conjugated poly(*p*-phenylenevinylene) (PPV) and a single acceptor layer of PAH labeled with either rhodamine B or fluorescein, it was shown that the FRET efficiency was dependent on the distance between the acceptor and donor according to the equation $1/(1 + (d_0/d)^4)$, where d is the distance between the acceptor and donor and d_0 is the critical energy transfer distance.[37] A similar observation was made by Schneider and Decher, where fluorescently labeled polymer layers separated from the gold nanoparticle core (quencher) by nonfluorescent polymer layers showed that fluorescence quenching through FRET was strongly distance-dependent.[38] In these studies, changes in the fluorescence intensities with new layer deposition or as a function of time were not investigated. Such information could yield useful knowledge over the extent of film rearrangement.

In this paper, we exploit FRET to gain a better understanding of the structure of DNA multilayer films on a molecular level. As illustrated in Scheme 1, the DNA multilayer films were assembled on amine-functionalized silica particles by depositing alternating layers of $polyA_{15}G_{15}$ and $polyT_{15}C_{15}$ onto a $polyT_{30}$ priming layer. The use of the $polyT_{30}$ priming layer ensures that when the next $polyA_{15}G_{15}$ layer is introduced, the $polyA_{15}$ block can hybridize to the T bases, leaving the $polyG_{15}$ block available for subsequent hybridization.[17] We have chosen tetramethyl-6-carboxyrhodamine-labeled (TAMRA) as the acceptor and Black Hole Quencher 2 (BHQ2) as the donor dye (Supporting Information S1). The advantage of using a BHQ rather than a fluorescent dye as an acceptor is because of its low fluorescence, which gives a high signal-to-noise ratio. To observe the efficiency of FRET within the films, $polyA_{15}G_{15}$-TAMRA (AG-F) donor and $polyT_{15}C_{15}$-BHQ2 (TC-Q) quencher layers were incorporated at various positions throughout the films (Scheme 2b−d). The fluorescence measurements were taken by measuring the average fluorescence intensity of 20 000 individual silica particles using flow cytometry.[40] This high throughput approach is well established for the analysis of FRET in cells[41] but is the first example (to our knowledge) in which flow cytometry has been used to analyze FRET in multilayer films.

EXPERIMENTAL SECTION

Materials. Sodium chloride (NaCl), sodium citrate, and sodium hydroxide were obtained from Sigma-Aldrich and used as received. High-purity water of resistivity greater than 18 MΩ cm was obtained from an inline Millipore RiOs/Origin system (Milli-Q water). A stock solution of saline sodium citrate (SSC buffer) was made up by dissolving 4.8 g of citric acid and 14.6 g of sodium chloride in 500 mL of water to give a final concentration of 500 mM NaCl and 50 mM sodium citrate (Na^+ concentration of 650 mM). The pH of the buffer solution was measured with a Mettler-Toledo MP220 pH meter and adjusted to pH 6.5 using 1 M sodium hydroxide. The oligonucleotides ($polyT_{30}$, $polyA_{15}G_{15}$, $polyT_{15}C_{15}$, and 5′-end-labeled TAMRA $polyA_{15}G_{15}$, abbreviated as AG-F) used were custom synthesized by Geneworks (Adelaide, Australia). $PolyT_{15}C_{15}$, internally labeled with Black Hole Quencher 2 (TC-Q), was synthesized by TriLink BioTechnologies (San Diego, CA). The lypophilized oligonucleotides were rehydrated in Milli-Q water to give a stock concentration of 150 μM. The concentrations of the oligonucleotide solutions were verified by measuring the absorbance at 260 nm (A_{260}) using an Agilent UV−vis 8453 spectrophotometer and calculated using the formula: oligonucleotide concentration = $A_{260}/\varepsilon_{260}$, where ε_{260} is the extinction coefficient of the single-stranded oligonucleotide. All stock oligonucleotide solutions were diluted in SSC buffer to a final concentration of 5 μM. Silica particles (2.59 ± 0.12 μm) were obtained from Microparticles GmbH (Umwelttechnologie-Zentrum, Germany) and amine-functionalized, as described previously.[18] Standard 5 MHz gold-coated AT-cut quartz crystals (Q-Sense AB, Västra Frölunda, Sweden) were cleaned with Piranha solution (70/30 v/v % sulfuric acid/hydrogen peroxide), washed thoroughly in water, and dried under a nitrogen stream. *Caution! Piranha solution is highly corrosive. Extreme care should be taken when handling Piranha solution, and only small quantities should be prepared.* All gold crystals were treated for 10 min in a UV-ozone TipCleaner (Bioforce NanoSciences, Inc.) to remove any remaining contaminants prior to the experiments.

Methods. *Quartz Crystal Microgravimetry.* QCM measurements were carried out on a Q-Sense E4 instrument (Q-Sense AB, Västra Frölunda, Sweden) at a constant temperature of 23.8 °C. All overtones measured (1st, 3rd, 7th, 11th, and 13th) showed the same trend; however, only the 5th overtone frequency and dissipation values are reported. The large dissipation changes observed throughout the film assembly indicate a highly swollen film,[17] which invalidate the assumptions in the Sauerbrey equation,[42] and hence the film buildup is qualitatively reported as a frequency change rather than absolute mass. Briefly, the unlabeled DNA film was assembled by first adsorbing a priming layer of $polyT_{30}$ (225 μL of a 5 μM solution for 10 min) onto the gold-coated quartz crystal electrodes, followed by alternating layers of $polyA_{15}G_{15}$ (225 μL of a 5 μM solution for 20 min) and $polyT_{15}C_{15}$ (225 μL of a 5 μM solution for 20 min) to a total of 11 layers (including the $polyT_{30}$ layer). The labeled film was assembled by depositing alternating layers of AG-F and TC-Q using the same protocol. Each film was rinsed in 1 mL of SSC buffer after each adsorption step to remove any loosely bound oligonucleotides. All solutions were flowed over the crystal sensor surface at a constant flow rate of 300 μL min^{-1}. The raw data were analyzed using the QTools 3.0.0.175 software.

Layer-by-Layer (LbL) Assembly of DNA Films on Silica Particles. The amine-functionalized silica particles (220 μL of a 5 wt % dispersion) were first primed with a $polyT_{30}$ layer (396 μL of a 5 μM solution). To assemble the layers, alternating layers of $polyA_{15}G_{15}$ (20 min) and $polyT_{15}C_{15}$ (20 min) were deposited. The amount of DNA used for subsequent layers was reduced proportionally to the number of particles taken out after each layer. After deposition of each layer, the particles were washed three times in SSC buffer to remove any excess DNA.

Flow Cytometry. The average fluorescence intensity of the particles was measured using a Partec FloMax space flow cytometer using an excitation wavelength of 488 nm (laser power 50 mW) and analyzed in the FL2 (564−606 nm) channel with a PMT voltage of 800 V. Analysis of flow cytometry data was performed using the Partec

FloMax software. The average fluorescence intensity of the particles over time was measured using a BD LSRFortessa flow cytometer using an excitation wavelength of 561 nm (laser power 50 mW). The 3 μm particles were analyzed with a 582/15 nm band-pass filter (574−590 nm) with a PMT voltage of 450 V. The signals obtained on different days were normalized by measuring the fluorescence intensity of eight peak Spherotech rainbow calibration particles. Analysis of flow cytometry data was performed using FlowJo software.

RESULTS AND DISCUSSION

The growth of a 30-mer diblock film assembled under 0.5 M salt concentration on particulate supports was followed by measuring the fluorescence intensity of the film labeled with an end-terminating TAMRA-labeled polyA$_{15}$G$_{15}$ layer (Scheme 2a), while using nonfluorescent layers to assemble the rest of the film. To study the efficiency of FRET, the DNA film was assembled by depositing an increasing number of non-fluorescent spacer layers between the fluorophore and quencher layers with no additional layers on top (Scheme 2b) or with additional layers on top of the quenched fluorophore (Scheme 2d). In particular, to understand whether rearrangement of the film could be induced by the formation of a new layer, nonfluorescent layers were deposited above the quenched fluorophore layer (Scheme 2c,d). The stability of the film over extended time periods was also monitored by following changes in the fluorescence intensity of the film over time. The efficiency of FRET in the films is reported by its quenching ratio (Q), which is defined as the fluorescence intensity of the quenched film divided by the fluorescence intensity of the unquenched film. The thickness between the layers, R, can be calculated using the Förster equation:

$$E = 1 - Q = \frac{1}{1 + \left(\frac{R}{R_0}\right)^6} \quad (1)$$

where E refers to the efficiency of energy transfer and R_0 is the Förster radius where the efficiency of energy transfer is 50%, theoretically calculated to be 4.4 nm (Supporting Information S2). Although studies have suggested using a spatial exponential of 4 instead of 6 for the calculation of E on planar supports, this equation holds only when the acceptor molecules are confined to ideal two-dimensional layers, which are separated from the donor layer by 3.5 nm and exist as a continuum.[37,39] However, in our study, we show that there is interpenetration and rearrangement of the layers within the DNA multilayer films, and thus these assumptions do not hold. Hence, we assume that the use of a spatial exponential of 6 as shown in eq 1 to be more appropriate in the calculation of E.

Influence of Labeled DNA on Film Growth. The growth of a diblock film (30-mer), monitored by QCM, has been reported in an earlier study.[17] The deposition of a polyA$_{15}$G$_{15}$ layer is generally characterized by a decrease in frequency (corresponding to an increase in film mass) and an increase in dissipation, while the polyT$_{15}$C$_{15}$ layer results in a frequency decrease and minimal change in dissipation.[17] In this study, as we used labeled polyA$_{15}$G$_{15}$ and polyT$_{15}$C$_{15}$, it was essential to determine whether the labeling of DNA building blocks with the fluorophore (TAMRA) or quencher (BHQ2) would have any influence on the growth of the film. As shown in Figure 1, a 5-bilayer DNA film assembled by depositing alternating layers of AG-F and TC-Q showed regular film growth. The film was found to have a higher dissipation and frequency change than the unlabeled film, suggesting a more swollen nature. This could be due to the presence of the hydrophobic fluorophore and quencher, which could reduce the efficiency of hybridization between the layers and result in a less stiff film (less double strands), as evidenced by the higher dissipation. However, in our experiments, as only two layers are labeled in each experiment, the influence of the fluorophore and quencher on film growth is expected to be minimal.

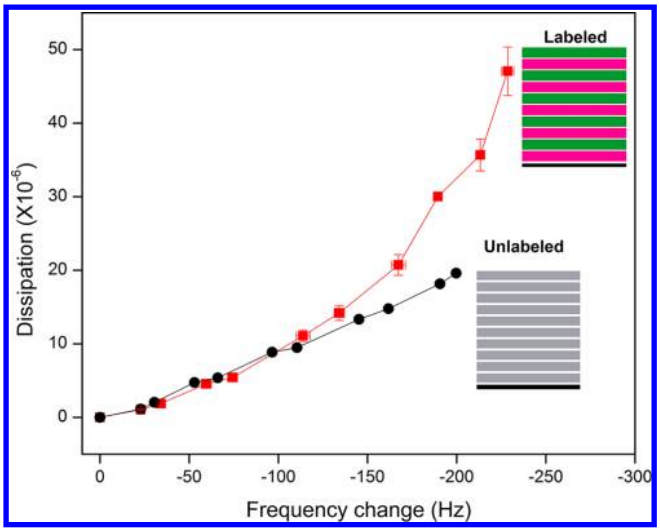

Figure 1. Comparison between the growth of a 5-bilayer labeled (polyT$_{30}$/(AG-F/TC-Q)$_5$) and unlabeled (polyT$_{30}$/(polyA$_{15}$G$_{15}$/polyT$_{15}$C$_{15}$)$_5$) film, as monitored using QCM. The polyT$_{30}$, TC-Q, and AG-F layers are represented by black, green, and pink lines, respectively.

Growth of DNA Films on Silica Particles. The growth of DNA films on 3 μm diameter silica particles was monitored by measuring the fluorescence intensity of the film after the deposition of a single AG-F layer at layers 1, 3, 5, 7, 9, and 11 (Figure 2). These layers correspond to every polyA$_{15}$G$_{15}$ layer within the 5-bilayer DNA film. As seen in Figure 2, the highest fluorescence intensity was observed for layer 1. This is possibly due to the electrostatic interactions between the initial AG-F layer with the positively charged amine-functionalized silica particle. An increase in fluorescence intensity for the subsequent layers (i.e., 3, 5, 7, 9, and 11) was observed and is mainly due to base-pairing interaction between the layers. These results are consistent with our previous findings on planar supports using dual polarization interferometry (DPI) where a higher mass of polyA$_{15}$G$_{15}$ was deposited during the first bilayer (ca. 1.6 ng mm^{-2}), followed by a lower but increasing mass of polyA$_{15}$G$_{15}$ for the subsequent second (0.4 ng mm^{-2}) to fifth bilayers (0.6 ng mm^{-2}) (Figure 2).[43] Through experimental and theoretical modeling we previously demonstrated that various multistranded structures such as branched DNA structures and T·A*T triplexes can form within the multilayer films.[20,43] It is important to note that the mass measured by DPI does not take into account the mass of water within the film and thus reflects only the mass of the DNA deposited. This confirms that deposition of DNA multilayer films on both planar and colloidal supports follow the same trend.

FRET in DNA Multilayer Films. The use of FRET to measure the distance between the fluorophore and quencher within a film can yield information about the molecular film structure, particularly over the sensitivity range between 2 and 10 nm. We assume that the distance between the fluorophore

dx.doi.org/10.1021/la302587t | Langmuir 2012, 28, 12527−12535

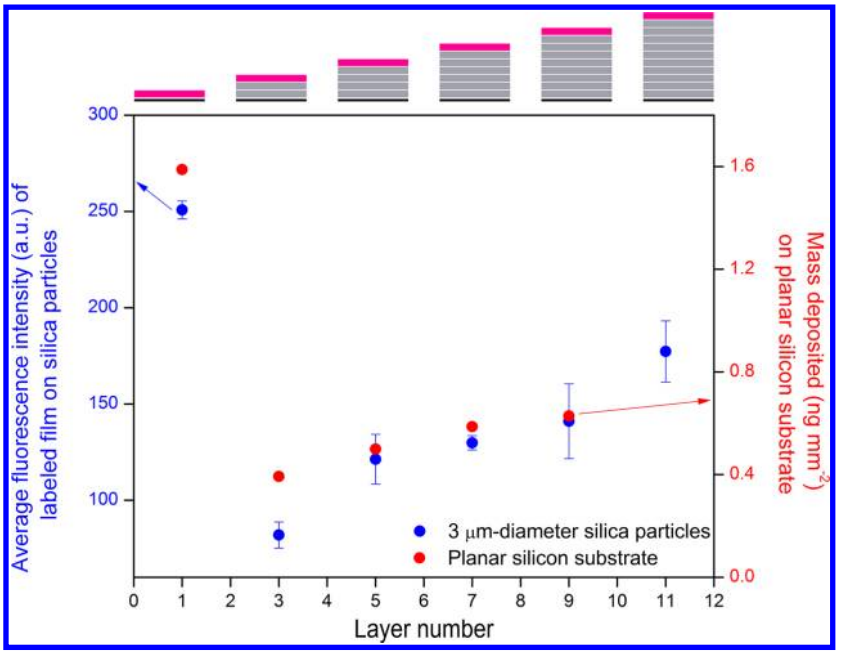

Figure 2. Growth of the DNA multilayer film by measuring the average fluorescence intensity of the film when capped with an AG-F layer (blue circles) and mass of polyA$_{15}$G$_{15}$ deposited (red circles) at different layer numbers. The schematic refers to fluorescently labeled films on the colloidal supports. The same film assembled on a planar silicon support was unlabeled.

and quencher is constant in the film and an average separation distance is obtained.

In the first set of experiments, the TC-Q quencher layer was fixed as the third layer and AG-F layers were introduced after the deposition of 0, 2, 4, 6, and 8 nonfluorescent layers. These data showed a steady increase in the quenched ratio as the number of nonfluorescent layers between the fluorophore and quencher was increased, as represented by the blue squares in Figure 3. This suggests, as expected, that the quencher is increasingly separated from the fluorophore as more nonfluorescent layers are introduced between them, thus restoring the fluorescence. When the quencher and fluorophore layers were placed directly above each other (Figure 3, layer number 0), a quenched ratio approaching 0 was observed. The fluorophore and quencher layers are separated by ca. 2 nm when they are directly above each other (see Supporting Information S3 and S4), and it is likely that at distances below 2 nm a ground-state complex forms, resulting in static quenching. However, as nonfluorescent layers were introduced between the quencher and fluorophore to increase their separation distance, the quenched ratio was seen to increase. The quenched ratio increased linearly from 0.15 when there were two layers between the fluorophore and quencher to 0.6 when there were eight layers separating them. This corresponds to a growing distance between the fluorophore and quencher layers with a separation distance of ca. 1 nm at zero layers to 5.3 nm at eight layers, as calculated using the Förster equation (1).

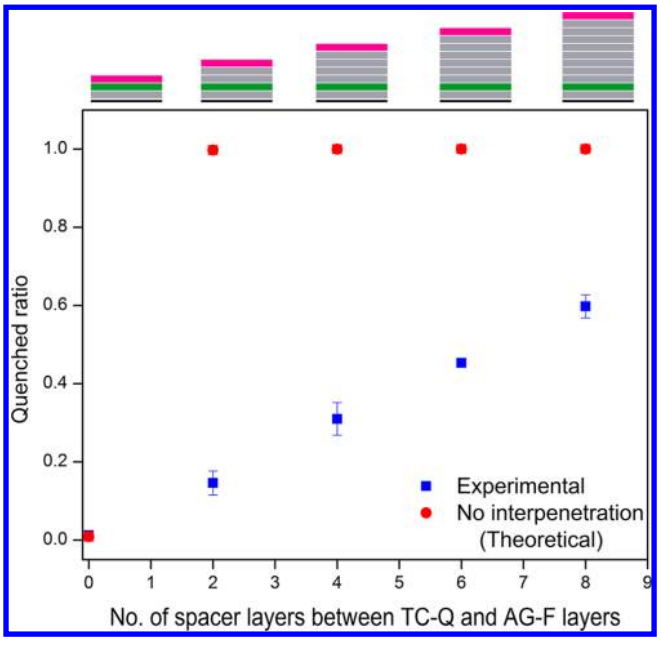

Figure 3. Quenched ratio of DNA multilayer films assembled by depositing alternating 0, 2, 4, 6, and 8 nonfluorescent spacer polyA$_{15}$G$_{15}$ and polyT$_{15}$C$_{15}$ layers between TC-Q and AG-F layers on polyT$_{30}$/polyA$_{15}$G$_{15}$ layers.

A theoretical quenched ratio of the DNA film with increasing nonfluorescent layers between the fluorophore and quencher was also calculated, assuming perfect stacking of the layers with no interpenetration (see calculations in Supporting Information S4). As seen in Figure 3, two nonfluorescent layers are theoretically sufficient to fully separate the fluorophore and quencher (quenched ratio ca. 1). Our experimental data at this point suggest that the fluorophore is still effectively quenched (quenched ratio ca. 0.15), suggesting rearrangement of the film brings the fluorophore and quencher closer together, resulting in effective quenching. Nonetheless, the experimental quenched ratio is observed to increase as more layers are introduced between the fluorophore and quencher, indicating that despite the rearrangement, the fluorophore and quencher can still be separated through the deposition of a sufficient number of nonfluorescent layers.

The extent of rearrangement during film assembly was also studied by monitoring changes in the quenched ratio as nonfluorescent layers were deposited above a quenched film

dx.doi.org/10.1021/la302587t | *Langmuir* 2012, 28, 12527−12535

with zero layers between the fluorophore and quencher layers. In the absence of any rearrangement, the film should remain quenched, and a constant quenched ratio of zero would be observed throughout the buildup (represented by the red dots in Figure 4). However, if the film undergoes 100% rearrangement such that there is uniform distribution of the layers (represented by the green triangles in Figure 4), the fluorophore and quencher would be separated after deposition of only three layers above the quenched fluorophore layer (see calculations in Supporting Information S5). Our experimental results (represented by black squares in Figure 4) show a linear increase in fluorescence intensity with layer deposition. The quenched ratio was close to zero when there were no layers above the quenched fluorophore layer, indicating total quenching. The quenched ratio increased to 0.3 after the deposition of seven nonfluorescent layers, which suggests that the rearrangement is not extensive. These results show that the hybridization process involved during formation of a new layer induces rearrangement of the film, which brings about separation of the quencher and fluorophore within the layers. The rearrangement of the film is unlikely to result in a loss of material, as our results (Figure 1 and previous work[17,18,20,43]) on the diblock film have shown that there is no film loss during the buildup process. The film likely rearranges during layer formation to achieve a new equilibrium state of stability, which is facilitated through slippage between the homopolymeric bases and interpenetration of the layers. Rearrangement has been reported to occur within electrostatically associated multilayer films[3,24,25,44] and is dependent on various factors, namely, the growth mechanism of the film (linear or exponential) and maintenance of the film electroneutrality (intrinsic or extrinsic charge compensation).[45] It has also been found recently that rearrangement can also occur in hydrogen-bonded films, where the absence of strong electrostatic interaction facilitates the stronger interpenetration of the polyelectrolytes within the hydrogen-bonded film network.[46] In an earlier study by Lavalle et al., it was suggested that the diffusion of polyelectrolytes within multilayer structures was dependent on the film permeability, in which films that were assembled using weakly charged polyelectrolytes and not tightly cross-linked were found to have an enhanced degree of interpenetrating layers.[27] DNA multilayer films are highly permeable structures, which are formed through slippage of the strands.[20] This, when combined with the lack of strong electrostatic interactions, could contribute to the rearrangement observed within the films during hybridization. More importantly, it implies that the rearrangement leads to a new stable film structure.

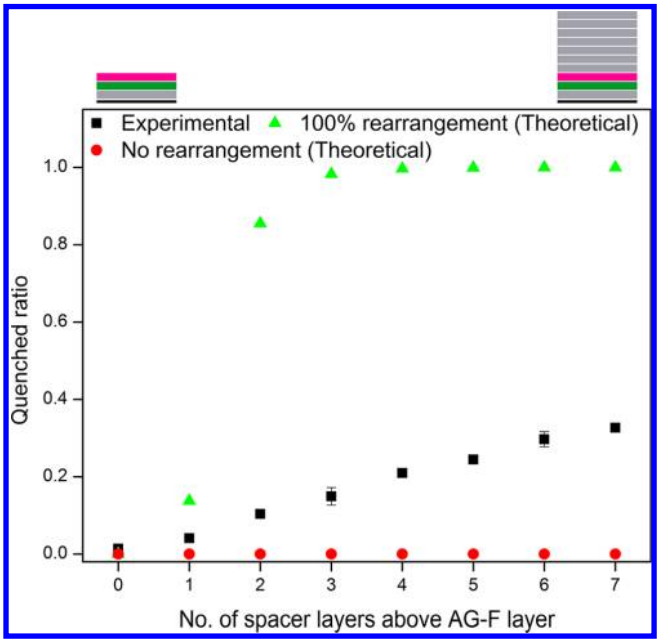

Figure 4. Quenched ratio of DNA film with increasing number of layers above the quenched fluorophore layers (represented by the black squares). The theoretical quenched ratio of the DNA film assuming 100% rearrangement and 0% rearrangement are represented by the green triangles and red circles, respectively. Layer 0 refers to a $polyT_{30}/polyA_{15}G_{15}$/TC-Q/AG-F film, and the subsequent odd and even numbers refer to a terminating $polyT_{15}C_{15}$ or $polyA_{15}G_{15}$ layer, respectively.

To investigate whether the structure of the film remained intact after assembly, additional nonfluorescent layers were also introduced above the fluorophore layer to a total of 5 bilayers in films where the fluorophore and quencher were separated by 0, 2, 4, and 6 layers. In the absence of any rearrangement, the fluorophore and quencher would remain intact within the layers; thus, the distance and hence quenched ratio between the two should remain constant. However, the results, represented by red dots in Figure 5, show an increase in the quenched ratio when additional layers were introduced. The addition of eight layers above the quenched film separated by zero layers ($x = 0$) led to an increase in the quenched ratio of 0.3, whereas the addition of two layers to the quenched film separated by six layers led to an increase in quenched ratio of 0.2 ($x = 6$). These results suggest that DNA films are dynamic structures and can undergo rearrangement. The structure of the film is thus not as ordered as illustrated in Scheme 1, but rather consists of

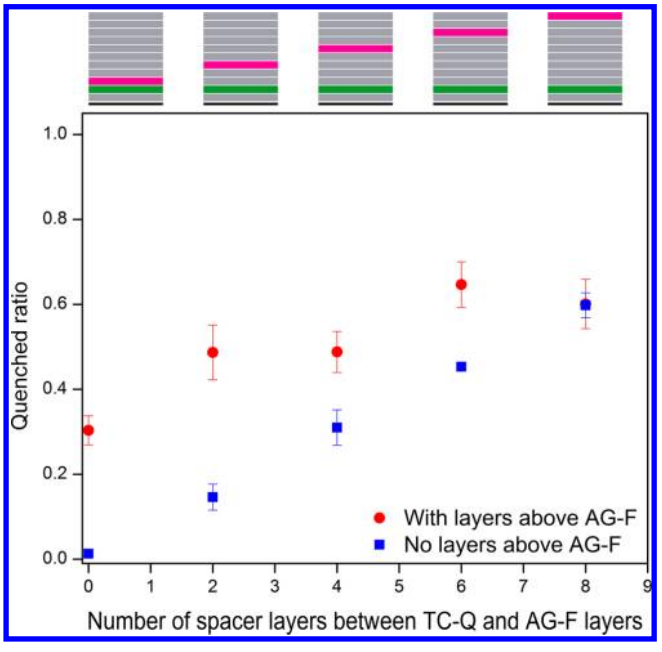

Figure 5. Quenched ratio of a 5-bilayer film with increasing number of layers between the TC-Q and AG-F layers (represented as red dots; scheme on top of plot). The blue squares represent the quenched ratio of the film with the same number of layers between the TC-Q and AG-F layers but without additional layers above the AG-F layer.

dx.doi.org/10.1021/la302587t | Langmuir 2012, 28, 12527−12535

interpenetrated layers due to the interpenetration and rearrangement of the layers during buildup.

Time Evolution of FRET in DNA Multilayer Films. A study was also carried out to examine the length of time required for rearrangement within the DNA films. In an earlier study on electrostatically held multilayer films, Picart et al.[25] reported that poly(L-lysine) (PLL) chains can diffuse within the PLL/hyaluronan (HA) multilayer film structure. It was later found that up to three populations of diffusing PLL polyelectrolyte chains could be identified: a fast diffusing, slow diffusing, and an immobile population.[24] In our experiments, two 5-bilayer DNA films with different fluorophore and quencher positions were studied: (1) where the fluorophore and quencher layers were separated by no layers, but with the addition of eight nonfluorescent layers above (Figure 6, Scheme 2d, where $a = 0$, $b = 8$), and (2) where there were eight nonfluorescent layers between the fluorophore and quencher layers with no additional terminating layers (Figure 6, Scheme 2d, where $a = 8$, $b = 0$). Our results showed that, in the first case, there was no significant change in the quenched ratio over time (Figure 6). These results suggest that while significant rearrangement of the layers occurred during hybridization of the layers deposited above the fluorophore (as shown in Figure 4), the resulting film has adopted a kinetically stable conformation. However, when the fluorophore and quencher were separated by eight nonfluorescent layers (with no capping layers), the quenched ratio of the film was observed to decrease over time. As seen in Figure 6, a decrease in the quenched ratio of ca. 25% over 120 h was observed. This suggests that the film slowly rearranges as the DNA strands rehybridize and diffuse through the highly permeable multilayer film. It is likely that the original conformation of this film results in a kinetically trapped structure that can rearrange over time, thus bringing the fluorophore and quencher closer together through dynamic rearrangement.

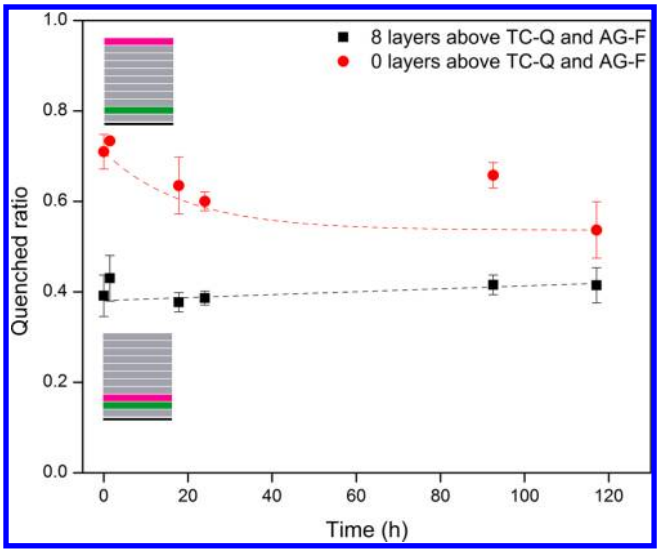

Figure 6. Quenched ratio of a 5-bilayer film (with no layers above the TC-Q and AG-F layers or with eight nonfluorescent layers above the TC-Q and AG-F layers) as a function of time. The dotted lines are to guide the eye.

CONCLUSIONS

We have shown using FRET that DNA films dynamically rearrange to achieve a stable state, which can be induced when a new layer is hybridized during assembly and also spontaneously over time. The incorporation of two to eight layers between the fluorophore and quencher led to a 4-fold increase in the quenched ratio, demonstrating that the incorporation of nonfluorescent layers between the fluorophore and quencher can be used to increase the distance between the fluorophore and quencher. However, because of rearrangement of the film during the hybridization process, this increase was less than theoretical predictions. We also showed that the deposition of nonfluorescent layers above the quenched fluorophore layer led to an increase in the quenched ratio, indicating that hybridization promotes rearrangement. The quenched ratio increased from 0 to 0.3 after the deposition of zero and seven layers, respectively. When the fluorophore and quencher are separated by eight nonfluorescent layers, the outermost fluorophore layer is able to diffuse through the film and stabilization is achieved over time. However, when eight nonfluorescent layers were deposited above the fluorophore layer, the quenched ratio remained constant over time. Our results suggest that DNA films are stable structures that can rearrange to form new film architectures when perturbed (during new layer formation) or spontaneously over time. We anticipate this study will be useful in engineering films for delivery and sensing applications, particularly where reusability of the film is of importance.

ASSOCIATED CONTENT

Supporting Information

Structures of TAMRA and BHQ2; Förster radius calculations; theoretical FRET calculations of a perfectly stacked film assembled using alternating poly$A_{15}G_{15}$ and poly$T_{15}C_{15}$ layers on a polyT_{30} primer layer; theoretical quenched ratio calculated using the distance between quencher and fluorophore with a varying number of nonfluorescent layers in between; and theoretical quenched ratio calculated using the distance between quencher and fluorophore with an increasing number of nonfluorescent layers above the quenched fluorophore, assuming rearrangement. This material is available free of charge via the Internet at http://pubs.acs.org.

AUTHOR INFORMATION

Corresponding Author

*E-mail fcaruso@unimelb.edu.au.

Notes

The authors declare no competing financial interest.

ACKNOWLEDGMENTS

We gratefully acknowledge the Australian Research Council for financial support (Discovery Project (DP0877360), Future Fellowship (FT110100265), and Federation Fellowship (FF0776078) schemes) and the Particulate Fluids Processing Centre for infrastructure support. The authors also acknowledge Samuel Lörcher for installation of the online Förster distance calculator.

REFERENCES

(1) Decher, G.; Hong, J. D.; Schmitt, J. Buildup of Ultrathin Multilayer Films by a Self-Assembly Process: III. Consecutively

Alternating Adsorption of Anionic and Cationic Polyelectrolytes on Charged Surfaces. *Thin Solid Films* **1992**, *210*−*211*, 831−835.
(2) Grigoriev, D. O.; Bukreeva, T.; Möhwald, H.; Shchukin, D. G. New Method for Fabrication of Loaded Micro- and Nanocontainers: Emulsion Encapsulation by Polyelectrolyte Layer-by-Layer Deposition on the Liquid Core. *Langmuir* **2008**, *24*, 999−1004.
(3) Decher, G. Fuzzy Nanoassemblies: Toward Layered Polymeric Multicomposites. *Science* **1997**, *277*, 1232−1237.
(4) Caruso, F.; Caruso, R. A.; Möhwald, H. Production of Hollow Microspheres from Nanostructured Composite Particles. *Chem. Mater.* **1999**, *11*, 3309−3314.
(5) Tjipto, E.; Cadwell, K. D.; Quinn, J. F.; Johnston, A. P. R.; Abbott, N. L.; Caruso, F. Tailoring the Interfaces between Nematic Liquid Crystal Emulsions and Aqueous Phases via Layer-by-Layer Assembly. *Nano Lett.* **2006**, *6*, 2243−2248.
(6) Mansouri, S.; Merhi, Y.; Winnik, F. M.; Tabrizian, M. Investigation of Layer-by-Layer Assembly of Polyelectrolytes on Fully Functional Human Red Blood Cells in Suspension for Attenuated Immune Response. *Biomacromolecules* **2011**, *12*, 585−592.
(7) Donath, E.; Moya, S.; Neu, B.; Sukhorukov, G. B.; Georgieva, R.; Voigt, A.; Bäumler, H.; Kiesewetter, H.; Möhwald, H. Hollow Polymer Shells from Biological Templates: Fabrication and Potential Applications. *Chem.—Eur. J.* **2002**, *8*, 5481−5485.
(8) Stockton, W. B.; Rubner, M. F. Molecular-Level Processing of Conjugated Polymers. 4. Layer-by-Layer Manipulation of Polyaniline via Hydrogen-Bonding Interactions. *Macromolecules* **1997**, *30*, 2717−2725.
(9) Zelikin, A. N.; Quinn, J. F.; Caruso, F. Disulfide Cross-Linked Polymer Capsules: En Route to Biodeconstructible Systems. *Biomacromolecules* **2006**, *7*, 27−30.
(10) Liu, Y.; Bruening, M. L.; Bergbreiter, D. E.; Crooks, R. M. Multilayer Dendrimer-Polyanhydride Composite Films on Glass, Silicon, and Gold Wafers. *Angew. Chem., Int. Ed.* **1997**, *36*, 2114−2116.
(11) Such, G. K.; Quinn, J. F.; Quinn, A.; Tjipto, E.; Caruso, F. Assembly of Ultrathin Polymer Multilayer Films by Click Chemistry. *J. Am. Chem. Soc.* **2006**, *128*, 9318−9319.
(12) Caruso, F.; Caruso, R. A.; Möhwald, H. Nanoengineering of Inorganic and Hybrid Hollow Spheres by Colloidal Templating. *Science* **1998**, *282*, 1111−1114.
(13) Städler, B.; Chandrawati, R.; Goldie, K.; Caruso, F. Capsosomes: Subcompartmentalizing Polyelectrolyte Capsules Using Liposomes. *Langmuir* **2009**, *25*, 6725−6732.
(14) Emoto, K.; Nagasaki, Y.; Kataoka, K. A Core-Shell Structured Hydrogel Thin Layer on Surfaces by Lamination of a Poly(ethylene glycol)-b-poly(D,L-lactide) Micelle and Polyallylamine. *Langmuir* **2000**, *16*, 5738−5742.
(15) Gao, M.; Richter, B.; Kirstein, S.; Möhwald, H. Electroluminescence Studies on Self-Assembled Films of PPV and CdSe Nanoparticles. *J. Phys. Chem. B* **1998**, *102*, 4096−4103.
(16) Johnston, A. P. R.; Read, E. S.; Caruso, F. DNA Multilayer Films on Planar and Colloidal Supports: Sequential Assembly of Like-Charged Polyelectrolytes. *Nano Lett.* **2005**, *5*, 953−956.
(17) Johnston, A. P. R.; Mitomo, H.; Read, E. S.; Caruso, F. Compositional and Structural Engineering of DNA Multilayer Films. *Langmuir* **2006**, *22*, 3251−3258.
(18) Lee, L.; Johnston, A. P. R.; Caruso, F. Manipulating the Salt and Thermal Stability of DNA Multilayer Films via Oligonucleotide Length. *Biomacromolecules* **2008**, *9*, 3070−3078.
(19) Singh, A.; Snyder, S.; Lee, L.; Johnston, A. P. R.; Caruso, F.; Yingling, Y. G. Effect of Oligonucleotide Length on the Assembly of DNA Materials: Molecular Dynamics Simulations of Layer-by-Layer DNA Films. *Langmuir* **2010**, *26*, 17339−17347.
(20) Lee, L.; Cavalieri, F.; Johnston, A. P. R.; Caruso, F. Influence of Salt Concentration on the Assembly of DNA Multilayer Films. *Langmuir* **2010**, *26*, 3415−3422.
(21) Johnston, A. P. R.; Caruso, F. Stabilization of DNA Multilayer Films through Oligonucleotide Crosslinking. *Small* **2008**, *4*, 612−618.
(22) Johnston, A. P. R.; Lee, L.; Wang, Y.; Caruso, F. Controlled Degradation of DNA Capsules with Engineered Restriction-Enzyme Cut Sites. *Small* **2009**, *5*, 1418−1421.
(23) Decher, G.; Lvov, Y.; Schmitt, J. Proof of Multilayer Structural Organization in Self-Assembled Polycation-Polyanion Molecular Films. *Thin Solid Films* **1994**, *244*, 772−777.
(24) Jourdainne, L.; Lecuyer, S.; Arntz, Y.; Picart, C.; Schaaf, P.; Senger, B.; Voegel, J.-C.; Lavalle, P.; Charitat, T. Dynamics of Poly(L-lysine) in Hyaluronic Acid/Poly(L-lysine) Multilayer Films Studied by Fluorescence Recovery after Pattern Photobleaching. *Langmuir* **2008**, *24*, 7842−7847.
(25) Picart, C.; Mutterer, J.; Richert, L.; Luo, Y.; Prestwich, G. D.; Schaaf, P.; Voegel, J.-C.; Lavalle, P. Molecular Basis for the Explanation of the Exponential Growth of Polyelectrolyte Multilayers. *Proc. Natl. Acad. Sci. U. S. A.* **2002**, *99*, 12531−12535.
(26) Schmitt, J.; Grünewald, T.; Decher, G.; Pershan, P.; Kjaer, K.; Lösche, M. Internal Structure of Layer-by-Layer Adsorbed Polyelectrolyte Films: A Neutron and X-Ray Reflectivity Study. *Macromolecules* **1993**, *26*, 7058−7063.
(27) Lavalle, P.; Picart, C.; Mutterer, J.; Gergely, C.; Reiss, H.; Voegel, J.-C.; Senger, B.; Schaaf, P. Modeling the Buildup of Polyelectrolyte Multilayer Films Having Exponential Growth. *J. Phys. Chem. B* **2004**, *108*, 635−648.
(28) Schlenoff, J. B.; Ly, H.; Li, M. Charge and Mass Balance in Polyelectrolyte Multilayers. *J. Am. Chem. Soc.* **1998**, *120*, 7626−7634.
(29) Dubas, S. T.; Schlenoff, J. B. Factors Controlling the Growth of Polyelectrolyte Multilayers. *Macromolecules* **1999**, *32*, 8153−8160.
(30) Sun, B.; Jewell, C. M.; Fredin, N. J.; Lynn, D. M. Assembly of Multilayered Films Using Well-Defined, End-Labeled Poly(acrylic acid): Influence of Molecular Weight on Exponential Growth in a Synthetic Weak Polyelectrolyte System. *Langmuir* **2007**, *23*, 8452−8459.
(31) Yoo, P. J.; Nam, K. T.; Qi, J.; Lee, S.-K.; Park, J.; Belcher, A. M.; Hammond, P. T. Spontaneous Assembly of Viruses on Multilayered Polymer Surfaces. *Nat. Mater.* **2006**, *5*, 234−240.
(32) Scholes, G. D. Long Range Resonance Energy Transfer in Molecular Systems. *Annu. Rev. Phys. Chem.* **2003**, *54*, 57−87.
(33) Marras, S. A. E.; Kramer, F. R.; Tyagi, S. Efficiencies of Fluorescence Resonance Energy Transfer and Contact-Mediated Quenching in Oligonucleotide Probes. *Nucleic Acids Res.* **2002**, *30*, e122.
(34) Huebsch, N. D.; Mooney, D. J. Fluorescent Resonance Energy Transfer: A Tool for Probing Molecular Cell-Biomaterial Interactions in Three Dimensions. *Biomaterials* **2007**, *28*, 2424−2437.
(35) Klitzing, R. V.; Möhwald, H. A Realistic Diffusion Model for Ultrathin Polyelectrolyte Films. *Macromolecules* **1996**, *29*, 6901−6906.
(36) Caruso, F.; Donath, E.; Möhwald, H. Influence of Polyelectrolyte Multilayer Coatings on Förster Resonance Energy Transfer between 6-Carboxyfluorescein and Rhodamine B-Labeled Particles in Aqueous Solution. *J. Phys. Chem. B* **1998**, *102*, 2011−2016.
(37) Richter, B.; Kirstein, S. Excitation Energy Transfer between Molecular Thin Layers of Polyphenylene Vinylene and Dye Labeled Polyallylamine in Layer-by-Layer Self-Assembled Films. *J. Chem. Phys.* **1999**, *111*, 5191−5200.
(38) Schneider, G.; Decher, G. Distance-Dependent Fluorescence Quenching on Gold Nanoparticles Ensheathed with Layer-by-Layer Assembled Polyelectrolytes. *Nano Lett.* **2006**, *6*, 530−536.
(39) Peralta, S.; Habib-Jiwan, J.-L.; Jonas, A. M. Ordered Polyelectrolyte Multilayers: Unidirectional FRET Cascade in Nanocompartmentalized Polyelectrolyte Multilayers. *ChemPhysChem* **2009**, *10*, 137−143.
(40) Johnston, A. P. R.; Zelikin, A. N.; Lee, L.; Caruso, F. Approaches to Quantifying and Visualizing Polyelectrolyte Multilayer Film Formation on Particles. *Anal. Chem.* **2006**, *78*, 5913−5919.
(41) Vereb, G.; Matkó, J.; Szöllósi, J. Cytometry of Fluorescence Resonance Energy Transfer. *Methods Cell Biol.* **2004**, *75*, 105−152.
(42) Sauerbrey, G. Verwendung von Schwingquarzen zur Wägung dünner Schichten und zur Mikrowägung. *Z. Phys.* **1959**, *155*, 206−222.

(43) Kato, N.; Lee, L.; Chandrawati, R.; Johnston, A. P. R.; Caruso, F. Optically Characterized DNA Multilayered Assemblies and Phenomenological Modeling of Layer-by-Layer Hybridization. *J. Phys. Chem. C* **2009**, *113*, 21185−21195.
(44) Baur, J. W.; Rubner, M. F.; Reynolds, J. R.; Kim, S. Förster Energy Transfer Studies of Polyelectrolyte Heterostructures Containing Conjugated Polymers: A Means to Estimate Layer Interpenetration. *Langmuir* **1999**, *15*, 6460−6769.
(45) Lavalle, P.; Voegel, J.-C.; Vautier, D.; Senger, B.; Schaaf, P.; Ball, V. Dynamic Aspects of Films Prepared by a Sequential Deposition of Species: Perspectives for Smart and Responsive Materials. *Adv. Mater.* **2011**, *23*, 1191−1221.
(46) Kharlampieva, E.; Kozlovskaya, V.; Ankner, J. F.; Sukhishvili, S. A. Hydrogen-Bonded Polymer Multilayers Probed by Neutron Reflectivity. *Langmuir* **2008**, *24*, 11346−11349.